MECHANOCHEMISTRY AND MECHANICAL ALLOYING 2003

JOURNAL OF MATERIALS SCIENCE **39** (2004) 5151–5154

Characterization of nanocrystalline Mn-Zn ferrites obtained by mechanosynthesis

T. VERDIER*, V. NIVOIX, M. JEAN, B. HANNOYER
LASTSM Université de Rouen, Institut des Matériaux, BP12, 76801 Saint Etienne du Rouvray Cedex, France
E-mail: thomas.verdier@univ-rouen.fr

Different Zn and Mn-Zn ferrites have been obtained by High Energy Ball Milling (HEBM) from elemental oxides. By varying the rotation speed of vials and main disk, several modes of milling can be obtained. In this paper, the materials prepared by two modes of milling, called shock (S) and high shock (HS), are studied by XRD and Mössbauer spectroscopy. Several mechanisms for spinel phase formation have been proposed. In particular, a reduction of Fe(III) occurs for the S mode, which leads to the formation of a wüstite-type phase which disappears after a long milling time. © *2004 Kluwer Academic Publishers*

1. Introduction

The High-Energy Ball Milling technique (HEBM) is applied in the field of synthesis of spinel ferrites. In some reports, after the HEBM, a thermal treatment is done to ensure the formation of fine-grained strained particles [1, 2]. This way of synthesis can induce changes in the distribution of cations in the spinel lattice [3, 4], which leads to unusual magnetic properties.

Mixed manganese zinc ferrites are materials of technological importance, widely used as transformers and inductors. They are usually synthesized at high temperature by solid state method. In this paper, their processing is performed in a high-energy planetary mill (Vario-Mill, Fritsch), which allows the vials and main disk velocities (ω and Ω (in rpm)) to be chosen independently. By varying the ratio of the velocities, it is possible to control the movements and trajectories of milling balls and consequently the nature of the end product. Based on two kinematic studies by Gaffet [5, 6], the different milling parameters are chosen to produce direct shock mode, intermediate mode or friction mode.

2. Experimental

The synthesis of Zn, Mn or Mn-Zn ferrite was accomplished by combining stoichiometric mixtures of powdered reactants such as ZnO, α-Fe_2O_3 and MnO obtained from ALFA AESAR (99% purity or better). The milling process was carried out under air atmosphere in a tempered steel vial (80 ml) with steel balls. A ball-to-powder weight ratio of 1:20 was used for two grinding modes, ($\Omega = 500$, $\omega = -500$) and ($\Omega = 600$, $\omega = -300$), which are called shock mode (S) and high shock (HS) mode, respectively. X-ray diffraction patterns were collected using a D-5000 powder diffractometer (Siemens) with CoK_α radiation. The Mössbauer measurements were performed in transmission geometry using ^{57}Co/Rh as γ-ray source. Mosfit software was used to analyse spectra [7].

3. Results

3.1. Mechanosynthesized zinc ferrite

Synthesis of zinc ferrite ($ZnFe_2O_4$) has been performed using several grinding conditions. The Fig. 1 shows the evolution of the ZnO/α-Fe_2O_3 mixture with the milling time for the S and HS modes. For the HS mode, a progressive disappearance of reactant oxide powders occurs in favour of a spinel phase which becomes pure after 12 h of milling. With S mode, disappearance of ZnO and α-Fe_2O_3 leads to simultaneous formation of a spinel phase and a wüstite-type phase (Fe, Zn)O. The latter phase disappears between 6 and 9 h of milling. The wüstite-type phase clearly shows the appearance of Fe(II) in the powders during the milling.

The zinc ferrite phases are obtained for both sets of grinding conditions, with a small amount of metallic iron originating from the wear of the milling equipment. However, the S mode is more efficient than the HS mode: using the S mode, the total disappearance of the starting oxides is reached within 9 h, whereas 12 h are necessary for the HS mode. The crystallite sizes of the obtained spinel phase (7 and 11 nm) and its cell parameters (0.8439 and 0.8438 nm) are similar for HS and S mode, respectively. These values are slightly lower than the cell parameter of a ceramic $ZnFe_2O_4$ (0.84411 nm , JCPDS file 22-1012).

In Fig. 2, the room temperature Mössbauer spectra of the materials obtained using the two different grinding modes are shown and compared with the spectrum of a ceramic $ZnFe_2O_4$. In the latter case, the spinel formula is $(Zn^{2+})_A(Fe^{3+}Fe^{3+})_BO_4^{2-}$, where A and B represent tetrahedral and octahedral sites, respectively. The

---

*Author to whom all correspondence should be addressed.

0022–2461

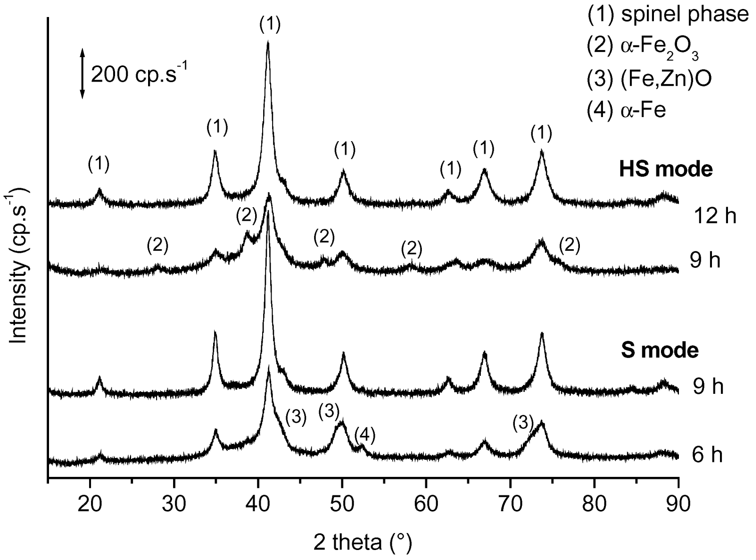

Figure 1 X-ray diffraction patterns of milled powder obtained by HS and S modes.

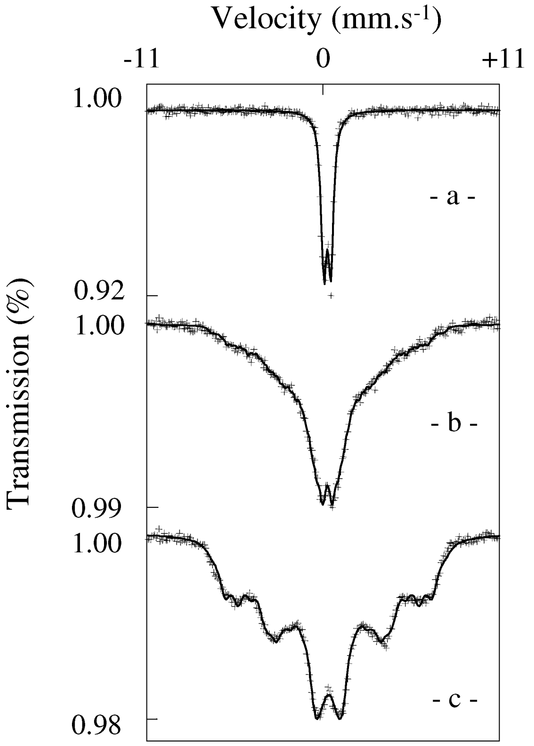

Figure 2 Room-temperature Mössbauer spectra of (a) $ZnFe_2O_4$ prepared by conventional thermal method, (b) powder obtained by HS mode (12 h), and (c) powder obtained by S mode (9 h).

TABLE I Hyperfine parameters of zinc ferrite obtained by HS mode (12 h) and S mode (9 h)

Grinding mode	IS (mm/s)	FWHM (mm/s)	2ε (mm/s)	Average HF (T)
HS (12 h)	0.36	0.92	0*	16.7
S (9 h)	0.41	0.88	−0.043	24.1

*Imposed value.

spectrum of ceramic $ZnFe_2O_4$ (Fig. 2a) is adjusted with a paramagnetic doublet with isomer shift of 0.35 mm/s and quadruple splitting of 0.44 mm/s. The spectrum of the material obtained using the HS mode (Fig. 2b) consists of a central doublet with a marked background curvature. The S mode spectrum (Fig. 2c) shows clearly the presence of magnetic features. The best fits for both spectra (Fig. 2b and c) are obtained using a distribution of hyperfine field (HF). In these fits the only variables of the sextet were isomer shift (IS), the quadrupole shift (2ε) and the line width (FWHM). Hyperfine parameters are presented in Table I.

Mössbauer results are in a good agreement with previously published data, i.e. the milled or mechanosynthesized zinc ferrite shows a broadened doublet compared to the ceramic phase. Several effects can explain the broadening of the doublet and the HF distribution required to fit the data. It can result either from a different repartition between the octahedral and tetrahedral sites of ions in the lattice, or from a grain size effect with a distribution of small particle sizes, or existence of strains and numerous defects induced by milling (or the three) [8, 9]. The kind of pattern shape of the S mode (Fig. 2c) has been observed in ceramic zinc ferrite containing Fe^{2+} ions [10, 11]. This means that the spinel ferrite obtained with the S mode contains iron (II).

The appearance of the wüstite-type phase in the early stages of grinding comes from several reactions. Previous papers have already shown that a reduction of Fe(III) is observed during milling with stainless steel vials and balls. Several mechanisms of the mechanically induced reduction processes are described, e.g., Kaczmarek and Ninham [12] explain that metallic-oxygen bonds can be broken by milling and then oxygen is removed, whereas Kosmac and Courtney [13] suggest a redox reaction between Fe(III) and metallic iron coming from the milling materials which leads to Fe(II). Sepelak *et al.* [14] conclude that the reduction process could be understood as a result of a short-time equilibration between spinel and the encrusted metallic iron phase of the milling tool during the impact period. They suggested that the minute quantities of abraded iron could play an initiating, catalytic role in the mechanochemical reduction processes. In the present study, the first mentioned mechanism is excluded because chemical analysis shows a gain of

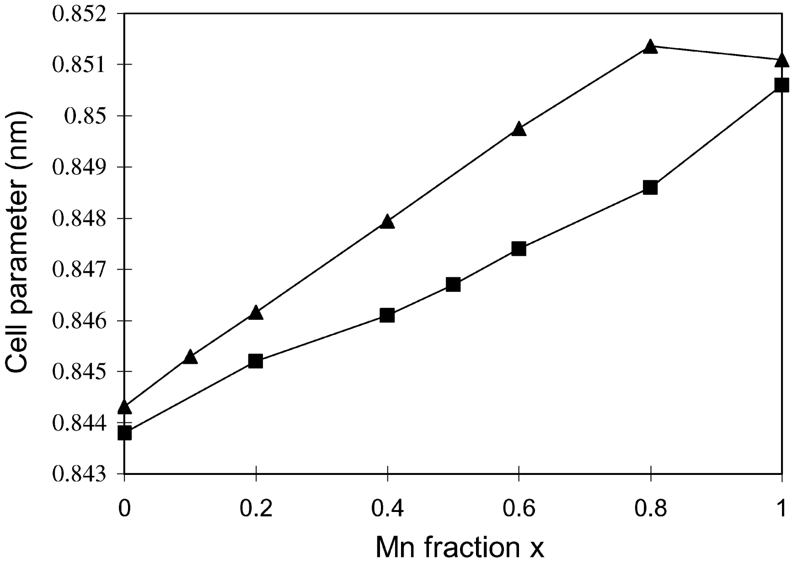

Figure 3 Cell parameter values of $Mn_xZn_{(1-x)}Fe_2O_4$ synthesised by ceramic route (▲) [16] and by mechanosynthesis (■).

iron during milling, correlated with a mass loss of the steel balls, and a slight decompression when opening the vials. In order to explain the appearance of the wüstite-type phase, two redox reactions can be considered, first between metallic iron from milling instruments and hematite or the second between metallic iron and zinc ferrite. To identify predominant reactions occurring during grinding, α-Fe_2O_3 and ceramic $ZnFe_2O_4$ are milled separately during 6 h using S mode. In this case, the presence of wüstite is not observed by XRD and Mössbauer spectroscopy. In order to examine the influence of zinc oxide on the formation of Fe(II), $ZnFe_2O_4$ and α-Fe_2O_3 are milled during 6 h using S mode, each of them with ZnO in the molar ratio 3:1. Mössbauer spectroscopy reveals that ZnO in addition to $ZnFe_2O_4$ does not contribute significantly to reduction of the spinel phase, whereas the milling of α-Fe_2O_3 with ZnO in the ratio 3:1 leads to the formation of three different phases: (i) a large amount of spinel phase, (ii) trace of iron and (iii) a small amount of non reacting α-Fe_2O_3. From the results of Mössbauer spectroscopy and value of cell parameter (0.8414 nm), the spinel phase can be identified as a zinc-substituted magnetite close to the formula $Zn^{2+}_{0.5}Fe^{2+}_{0.5}Fe^{3+}_2O^{2-}_4$ [15]. This result indicates that a reduction of Fe(III) by Fe takes place, reaction which is favoured by the presence of ZnO. The formation of the zinc ferrous ferrite can be understood as the two-steps process which includes the formation of an intermediate solid solution (Fe, Zn)O and its subsequent reaction with remaining hematite. It should be noted that a solid solution (Fe, *Me*)O with wüstite structure has already been obtained as the result of the mechanochemical reduction of $MeFe_2O_4$ (*Me* = Mg, Ni) [14, 16]. Similarly, Kosmac and Courtney [13] have also observed the formation of the solid solution (Fe, Zn)O during milling of α-Fe_2O_3 and ZnO.

The milling parameters seem to have a real influence on the nature of the obtained phases: a very high shock mode leads to a zinc ferrite close to a material prepared usual ceramic compound, whereas shock mode, by a reaction with iron, causes a reduction of Fe(III) with the appearance of Fe(II), first in a wüstite-type phase, and finally incorporated in a spinel phase.

3.2. Mechanosynthesized Mn-Zn ferrite

Pure Mn-Zn ferrites $Mn_xZn_{(1-x)}Fe_2O_4$ are synthesized using the S milling mode within 9 h of milling. The values of the cell parameter of the obtained spinel phases are displayed in Fig. 3, in comparison with the literature data [17]. The results show a good agreement for extreme x values but they are different for intermediate composition. Differences may come from a change of the cation distribution, which leads to a change of the cell parameter [18].

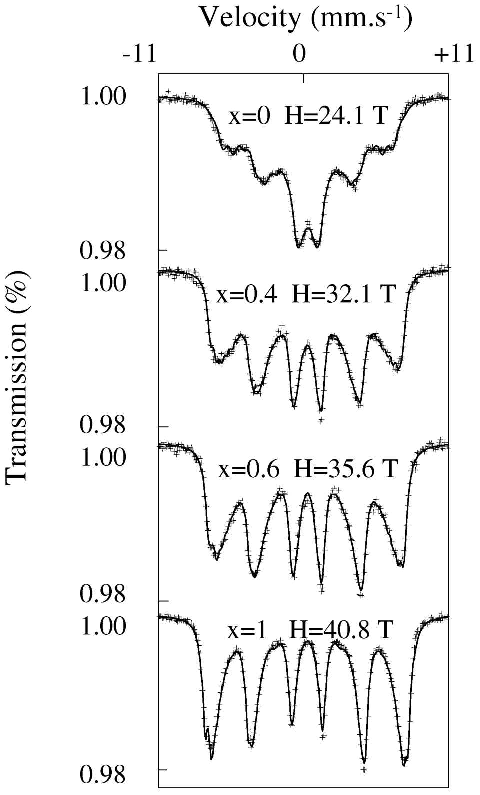

Figure 4 Room-temperature Mössbauer spectra of manganese-zinc ferrites $Mn_xZn_{(1-x)}Fe_2O_4$ obtained by S mode for 9 h.

The room temperature Mössbauer spectra of the prepared $Mn_xZn_{(1-x)}Fe_2O_4$ phases (Fig. 4) consist of broadened sextet that are clearly indicative of the distribution of hyperfine fields with a gradual change as the zinc concentration decreases (average hyperfine field values are displayed in Fig. 4). It is well known that in mixed manganese zinc ferrites, the following equilibrium occurs : $Fe^{3+} + Mn^{2+} \Leftrightarrow Fe^{2+} + Mn^{3+}$ [19]. The way of synthesis governs the shifting of this equilibrium, so it defines the cation distribution and consequently the magnetic properties [20–22]. In the present study, Fe(II) may also come from a redox reaction between Fe(III) and metallic iron, as it has been observed previously in zinc ferrite. For a 6 h grinding, no wüstite phase is observed, but the redox reaction can not be excluded. The existence of multiple elements present under several valencies and the small particle size make the room-temperature Mössbauer study of this system difficult.

4. Conclusion

First results on the mechanochemical preparation of materials using the new Vario-Mill are very promising: the possibility of changing the milling parameters leads to the obtaining of several types of spinel ferrites, different from the usual ceramic powders. Furthermore, the iron from the milling material has a strong influence on the synthesis. It could be interesting to make experiments with WC balls and vials.

Acknowledgements

One of the authors, T.V. thanks the Région Haute Normandie for financial assistance.

References

1. S. D. SHENOY, P. A. JOY and M. R. ANANTHARAMAN, *J. Magn. Magn. Mater.* **269** (2004) 217.
2. N. GUIGUE-MILLOT, S. BEGIN-COLIN, Y. CHAMPION, M. J. HYTCH, G. LE CAËR and P. PERRIAT, *J. Solid State Chem.* **170** (2003) 30.
3. D. J. FATEMI, V. G. HARRIS, V. M. BROWNING and J. P. KIRKLAND, *J. Appl. Phys.* **83** (1998) 6867.
4. H. EHRHARDT, S. J. CAMPBELL and M. HOFMANN, *J. Alloys Compd.* **339** (2002) 255.
5. M. ABDELLAOUI and E. GAFFET, *ibid.* **209** (1994) 351.
6. *Idem.*, *Acta Materiala* **43** (1995) 1087.
7. J. TEILLET, F. VARRET and J. JURASZEK, unpublished software.
8. J. Z. JIANG, P. WYNN, S. MORUP, T. OKADA and F. J. BERRY, *Nanostruct. Mater.* **12** (1999) 737.
9. V. SEPELAK, U. STEINIKE, D. C. UECKER, S. WI[SS]MANN and K. D. BECKER, *J. Solid State Chem.* **135** (1998) 52.
10. D. C. DOBSON, J. W. LINNETT and M. M. RAHMAN, *J. Phys. Chem. Solids* **31** (1970) 2727.
11. C. M. SRIVASTAVA, S. N. SHRINGI and R. G. SRIVASTAVA, *Phys. Rev.* B **14** (1976) 2041.
12. W. A. KACZMAREK and B. W. NINHAM, *IEEE Trans. Magn.* **30** (1994) 732.
13. T. KOSMAC and T. H. COURTNEY, *J. Mater. Res.* **7** (1992) 1519.
14. V. SEPELAK, M. MENZEL, K. D. BECKER and F. KRUMEICH, *J. Phys. Chem.* B **106** (2002) 6672.
15. C. M. SRIVASTAVA, S. N. SHRINGI, R. G. SRIVASTAVA and N. G. NANADIKAR, *Phys. Rev.* B **14** (1976) 2032.
16. M. MENZEL, V. SEPELAK and K. D. BECKER, *Solid State Ionics* **141/142** (2001) 663.
17. V. U. KONIG and G. CHOL, *J. Appl. Cryst.* **1** (1968) 124.
18. P. POIX, *Sem. Etat Solide* **1** (1966) 82.
19. K. KLEINSTÜCK, E. WIESER, P. KLEINERT and R. PERTHEL, *Phys. Stat. Sol.* **8** (1965) 271.
20. A. H. MORRISH and P. E. CLARK, *Phys. Rev.* B **11** (1975) 278.
21. L. CSER, I. DÉZSI, I. GLAGKIH, L. KESZTHELYI, D. KULGAWCZUK, N. A. EISSA and E. STERK, *Phys. Stat. Sol.* **27** (1968) 131.
22. M. EL GUENDOUZI, K. SBAI, P. PERRIAT and B. GILLOT, *Mater. Chem. Phys.* **25** (1990) 429.

Received 11 September 2003
and accepted 27 February 2004